# JET Intrinsic Rotation Studies in Plasmas with a High Normalised Beta and varying Toroidal Field Ripple

M.F. F. Nave[1, 2], L.-G. Eriksson[3], C. Giroud[4], T. Johnson[5], K, Kirov[4], M.-L. Mayoral[4], J-M Noterdaeme[6, 7], J. Ongena[8], G. Saibene[9], R. Sartori[9], F. Rimini[4], T. Tala[10], P. de Vries[11], K-D Zastrow[4] , JET-EFDA Contributors[*]

*JET-EFDA, Culham Science Centre, OX14 3DB, Abingdon, UK*

[1]*Associação EURATOM/IST, Instituto de Plasmas e Fusão Nuclear, Instituto Superior Técnico, Universidade Técnica de Lisboa,, P1049-001, Lisbon, Portugal*

[2]*Rudolf Peierls Centre for Theoretical Physics, Oxford University, Oxford, UK*

[3]*European Commission, Research Directorate General, B-1049 Brussels, Belgium*

[4]*Euratom/CCFE, Culham Science Centre, OX14 3DB, Abingdon, U.*

[5]*Association EURATOM - VR, Fusion Plasma Physics, EES, KTH, Stockholm, Sweden*

[6]*Max-Plank-Institut fur Plasmaphysik, Garching, Germany*

[7]*EESA Department, UGent, Gent, Belgium*

[8]*ERM-KMS, Association EURATOM-Belgian State, Brussels, Belgium, TEC Partner*

[9]*Fusion For Energy Joint Undertaking, Barcelona, Spain*

[10]*VTT Association Euratom-Tekes, VTT, Finland*

[11]*FOM Institute for Plasma Physics, Rijnhuizen, Association EURATOM-FOM, Nieuwegein, the Netherlands*

[*]*See the Appendix of F. Romanelli et al., Proc. of the 23rd IAEA FEC2010, Daejeon, Korea*

## Abstract

Understanding the origin of rotation in Ion Cyclotron Resonance Frequency (ICRF) heated plasmas is important for predictions for burning plasmas sustained by alpha particles, being characterized by a large population of fast ions and no external momentum input. The angular velocity of the plasma column has been measured in JET H-mode plasmas with pure ICRF heating for both the standard low toroidal magnetic ripple configuration, of about ~ 0.08% and, for increased ripple values up to 1.5 % [1]. These new JET rotation data were compared with the multi-machine scaling of ref. [2] for the Alfven-Mach number and with the scaling for the velocity change from L-mode into H-mode. The JET data do not fit well any of these scalings that were derived for plasmas that are co-rotating with respect to the plasma-current. With the standard low ripple configuration, JET plasmas with large ICRF heating power and

normalized beta, $\beta N \approx 1.3$, have a very small co-current rotation, with Alfven-Mach numbers significantly below those given by the rotation scaling of ref. [2]. In some cases the plasmas are actually counter-rotating. No significant difference between the H-mode and L-mode rotation is observed. Typically the H-mode velocities near the edge are lower than in L-modes. With ripple values larger than the standard JET value, between 1% and 1.5%, H-mode plasmas were obtained where both the edge and the core counter rotated.

## I - Introduction

Intrinsic rotation can play a key role in the performance of future tokamak power plants where the momentum input will be small [3]. In present day tokamak experiments, rotation is mostly driven by the torque coming from the neutral beam injection (NBI). However, in reactors with high NBI power at high beam energy, the torque is expected to be small. The central toroidal rotation velocity for ITER H-mode plasmas with NBI power of 34 MW, was predicted to be in the range of 10-170 km/s [4]. This is lower than currently observed at JET for the same Prandtl number (ratio between momentum and ion heat diffusivity) and with NBI power less than 20 MW [5]. It is important to note that ITER simulations depend on options of momentum transport whose theory is still evolving. For instance, the ITER simulations of ref. [4] do not include any contribution from a momentum pinch which is found to exist in JET NBI discharges [6, 7] and other tokamaks [8, 9]. This inward pinch will modify the rotation profile in ITER, in particular the peaking of the rotation profile will increase. Understanding of momentum transport is crucial in order to reliably model rotation profiles in ITER and other future devices, however, this is not the scope of this paper. A good overview of momentum transport theory, covering also aspects like residual stress and up-down asymmetry that may affect significantly the rotation profile in ITER, is given in reference [10].

As the NBI driven rotation in future machines is presumed to be small, the intrinsic plasma rotation, which occurs in the absence of momentum sources such as NBI, has created a lot of interest. The question of whether intrinsic rotation would on its own or as a supplement to NBI induced rotation be sufficient to fulfill the requirements for high confinement plasmas such as the suppression of turbulence and stabilization of MHD modes is a key issue. For predictions for future machines which will be larger than the present ones, it is important to assess the scaling of the intrinsic rotation with machine size, in particular for resistive-wall mode mitigation. The 2007 paper of J. Rice et al [2] was an important attempt in this

direction. From the extrapolation of intrinsic plasma rotation data observed in several machines it was predicted that a substantial co-rotation, i. e. in the direction parallel to the plasma current, would occur in ITER. This extrapolation based on the fitting of rotation data from six machines (Alcator C-Mod, DIII-D, JET, JT-60, Tore-Supra and TCV) produced what is currently know in the controlled nuclear fusion community as the "Rice scaling": a scaling for the Alfven-Mach number, $M_A$ ($=V_\phi/C_A$, where $C_A$ is the Alfven velocity) using the measured intrinsic toroidal velocities, $V_\phi$, during enhanced plasma confinement regimes and, a scaling for the difference between toroidal velocities, $\Delta V_\phi$, measured in enhanced and L-mode phases. At that time, the JET intrinsic rotation database was rather limited and only two JET pulses were included in that study. Since the variation of the plasma parameters of the two JET pulses was small, e.g., they had the same plasma current, $I_p$, and similar values of the parameter $\beta$ (the ratio of thermal to magnetic plasma pressure), it was not clear how well a more extensive JET data set would fit a scaling where rotation was found to depend on $\beta$ and $I_p$. In order to further contribute to this multi-machine intrinsic rotation study, a database of JET H-mode plasmas with pure Ion Cyclotron Resonance Frequency (ICRF) heating and for which the toroidal angular velocity of the plasma column was measured, has been built. This database includes ELM-free and ELMy plasmas done in 1994-95 with normalized plasma pressure levels, $\beta_N$, up to 0.7 [11] (the ELM-free plasmas were used as JET input in the rotation scalings of ref. [2]) and post 2000 data with $\beta_N$ up to 1.3, from ELMy H-modes from a study performed in 2000 as reported in [12] and, data from 2009 experiments not previously reported. The database also includes pulses with different magnetic field ripple , $\delta_{TF}$ (where $\delta_{TF}=(B_{max}-B_{min})/(B_{max}+B_{min})$, with $B_{max}$ and $B_{min}$ being the maximum and minimum toroidal field values). The effect of the magnetic field ripple on intrinsic rotation was assessed with $\delta$ values ranging from $\delta_{TF}$ ~0.08%, which is the JET standard low ripple configuration, to an enhanced $\delta_{TF}$ up to 1.5% [1].

All the experiments reported here are from Deuterium plasmas using Hydrogen minority ICRF heating with the H fundamental cyclotron resonance layer, $R_{res}$, located near the centre. In all them, the ICRF power was coupled using the four A2 antennae [13], known as antennas A, B, C, and D. In pulses performed in 2009, additional power was provided by the JET ICRF ITER-Like antenna (ILA) [14]. The antennae layout is illustrated in figure 1. Both the A2s and the ILA antennae were used in a dipole phasing i.e. such that the launched waves have a symmetric toroidal mode number spectrum. Note that due to the recent modifications made

on the A2 ICRF systems and the addition of the ILA, the averaged ICRF power that can be coupled on type I ELMy H-mode has greatly increased and that ICRF is now commonly used in combination with NBI heating in JET H-mode experiments [15, 16]. Because of this improvement, very steady and reliable ICRF power was coupled in 2009 experiments with dominant ICRF power [24] and in a few cases with pure- ICRF power.

It is important to note the effect that the ICRF heating scheme and the antenna phasing can have on the rotation. With minority heating and an asymmetric phasing (i.e. either $+90^0$ phasing resulting in launched waves propagating predominantly in the co-current direction or $-90^0$ phasing resulting in launched waves propagating predominantly on the counter-current direction), a small toroidal momentum in either co- or counter-current can be produced and consequently small effects on the core rotation (~3 krad/s) observed [12]. In the case of minority heating it was also shown that the minority resonance layer position can have an effect on the core rotation [1, 12], as has the minority level [17]. Enhanced rotation is also observed when using an ICRF mode-conversion heating scheme as shown in recent experiments in C-Mod [18] and in JET, where counter-rotation in the core of JET L-mode plasmas, up to a modest value of 10 krad/s, was observed [19]. Note that most of these results were from L-mode plasmas. In this paper only H-mode plasmas with no net ICRF wave-momentum input (i. e. with no asymmetric antenna phasing and no mode-conversion) are considered.

In this paper, we first give an overview of the rotation measurement techniques (section IIa) and an overview of the measurements of intrinsic rotation in H-mode plasmas, in the usual low ripple configuration (section IIb) and with larger ripple (section IIc). A comparison with the multi-machine rotation scalings of ref. [2] is presented in section III and the conclusions follow in section IV.

## II - Observations

### IIa - Tools for measuring intrinsic rotation

Intrinsic rotation in JET plasmas can be determined from X-ray crystal spectroscopy (XCS) [20], from charge exchange recombination spectroscopy (CXRS) [21, 22] and, from the observed frequency of MHD modes [17]. These three methods of diagnosing the toroidal rotation, give comparable angular rotation velocities.

The toroidal angular frequency in the plasma core can be obtained with a high-resolution X-ray crystal spectrometer (XCS) that observes the spectrum around the resonance line of the

helium-like nickel ion $Ni^{+26}$ . This is a passive technique ideal for measuring rotation in plasmas with pure ICRF heating, however it only gives information at one radial position, the localization depending on the plasma temperature. Early JET intrinsic rotation studies have used this technique [11, 23]. The JET intrinsic rotation data included in the multi-machine study of [2] is from XCS measurements from 1994-95, when the wavelength scale had for the first time been calibrated by comparison with the angular frequency derived during NBI from charge exchange recombination spectroscopy of $C^{+6}$ . For newer pulses XCS intrinsic rotation measurements are not always available as there isn't enough Ni in the JET machine in X-point plasmas.

Since the year 2000, intrinsic rotation angular frequency profiles have been measured by CXRS using the "NBI blip" technique [12]. CXRS measurements, with an integration time of 10 ms, are taken during short NBI pulses with typical duration of 100-200 ms and $P_{NBI}$~1-2 MW. In the normal JET configuration, i.e. $\vec{B}_T//\vec{I}_p$ (see figure 1) and the usual low toroidal field ripple, NBI provides a toroidal momentum source in the direction of the plasma current. The geometry of the line of sight of the CXRS diagnostic and the intersecting beam lines are shown schematically in figure 1. To determine the rotation of plasmas with ICRF heating, only CXRS measurements taken within the first few tens of ms are used, when rotation driven by NBI is still negligible [12].

The velocity of the toroidal rotation is determined from the Doppler shift of the active charge exchange spectrum of $C^{+6}$. The $Be^{1+}$ emission line at 527.063nm is used as a reference wavelength as it is assumed non-rotating in the cold scrape-off-layer. There are two ways of processing the spectra in order to deduce the toroidal rotation velocity. Results of both analyses are presented here. The first method uses multi-Gaussian fit to the $C^{+6}$ emission line [22]. Two Gaussian fit function accounts for: (i) the 'warm' component, which is due to charge exchange between $C^{+6}$ ions and thermal deuterium at the edge and (ii) the 'hot' component which arises from the interaction of the $C^{+6}$ with the fast neutral beam. This method works well when there is a large difference between edge and core temperature and rotation, because under this condition the two components ('warm' and 'hot') are clearly distinguished from each other in a least square fit. When this condition is not met as for instance in plasma with low momentum input, in which cases core temperature and rotation are very similar, then the spectra become difficult to analyse and the second method was used. In this case the spectra taken during the diagnostic NBI blip are subtracted from the spectrum taken just before the application of beam power. The so called subtracted spectra are analysed

by fitting them to only one Gaussian component. Statistical errors, determined from the error in the least square fit [22], are shown as shaded areas in the plots below. CXRS intrinsic rotation measurements have been routinely compared with the observed frequency of MHD modes [1, 12, 17] which have always confirmed the direction of rotation and measured rotation frequencies in the core of the plasma. A benchmark of XCS, CXRS and MHD observations for ICRF L-mode plasmas has showed that all three methods give comparable angular rotation velocities.

**II b - Rotation studies in H-mode plasmas with low magnetic filed ripple configuration**

Most of the JET intrinsic rotation measurements with pure ICRF minority heating are from L-mode plasmas obtained under various conditions: for different ICRF resonance positions, for various symmetric and asymmetric k// spectra of the antenna and, with different minority concentrations. The L-mode observations are summarized in references [12, 17]. With its usual low ripple value, JET L-mode plasmas with ICRF heating are observed to rotate with small toroidal angular frequencies, typically less than $\omega_\phi \leq 10\,\mathrm{krad/s}$. The L-mode edge is clearly always co- rotating, while the core is either counter- or co-rotating depending on the plasma current [17], and heating details [12, 17]. The observed rotation angular frequencies in L-mode plasmas show no correlation with ICRF power and no correlation with the normalized beta parameter, $\beta_N$ [17].

The JET intrinsic rotation database in H-mode plasmas with pure ICRF heating has few pulses, which is due in part to the JET experimental priorities and in part to the initial technical difficulties in maintaining a steady ICRF heating power in H-mode plasmas with edge localized modes (ELMs). As mentioned above, JET has now an ELM resilient ICRF system. Its use for intrinsic rotation studies has just started to be explored. The current database of rotation measurements in H-mode plasmas with pure ICRF heating, from where examples will be shown in this section, includes ELM-free and ELMy plasmas done in 1994-95 with $\beta_N$ levels up to 0.7 [11] and more recent data obtained in ELMy discharges with $\beta_N$ values up to 1.3. Since the observed core rotation may depend on SOL parameters, one should note that the 1994-95 plasmas were obtained with the then newly installed divertor Mark I [25], while subsequent measurements come from plasmas with more closed divertors.

In the early 1994-95 experiments in ELM-free H-mode plasmas [11], co-rotation with angular frequencies up to 23 krad/s ( $v_\phi$ ~70 km/s) were measured with XCS in the core of the plasma at a normalised radius $\rho = 0.39 \pm 0.1$ (the central localization corresponding to a major radius R=3.5 m, just outside the sawtooth inversion radius), with ICRF power $P_{ICRF}$ ~ 5 MW, as shown in figure 2. Co-rotation increased after the L-H transition (at t~18.9 s ), until it was limited by a combination of core and edge MHD modes. This pulse is one of the two JET pulses included in the multi-machine scalings of reference [2]. Co-rotation, however, was not a characteristic of all early JET ICRF H-modes, as illustrated in fig. 7 of [11] where $\omega_\phi$ decreased and counter-rotation was observed in the H-mode phase. Two differences were then pointed out with respect to the co-rotating cases, a higher recycling and the presence of frequent regular ELMs.

The high co-rotation values, and clear difference between rotation frequencies in H-mode and L-mode (as in figure 2), have not been observed in subsequent experiments. In the ELMy H-modes reported in [12] and the new experiments reported here, no significant differences in the range of measured angular frequencies in L-mode and H-mode were found. In some cases the edge was found to counter-rotate [12]. The following two examples show plasmas with higher coupled ICRF powers in ELMy H-modes.

In view of the present study, particular attention was given to a pulse from experiments performed in the year 2000 [12], for which up to 10 MW of ICRF power was coupled to an ELMy H-mode. The time evolution for this pulse is shown in figure 3, where the ICRF power is ramped up from an initial phase with 2MW to 10MW. CXRS rotation measurements were taken during diagnostic blips in phases with ICRF-only at t=18.32 s (L-mode with $P_{ICRF}$~2MW) and at t= 24.02 s (ELMy H-mode with $P_{ICRF}$ ~10MW) and during a continuous NBI phase, from t=19.7 s to t=21.6 s, with $P_{NBI}$~2 MW. It is during the continuous NBI phase, when $P_{ICRF}$ was increased to 6 MW that the L-H transition occurred, at t=20.78 s, as indicated by a sharp increase in the edge $T_e$ gradient. This continuous NBI phase shows the effect of an increase in ICRF power on rotation. As observed in many pulses, in L-mode the effect is mostly to decrease the edge rotation until the L-H transition. After the L-H transition, rotation increases both in the plasma centre and at the edge but only until the appearance of a large MHD event such a sawtooth or the first ELM. The edge rotation remains at a level lower than observed in the ELM-free phases once regular ELMs start (in close up in figure 6). The angular frequency measured later in the ICRF-only phase (at t= 24.02 s), when $\beta_N$~1.3, shows that the H-mode edge is slightly counter-rotating. Another example of edge counter-rotation is

shown in fig. 18 of reference [12], where edge counter-rotation was reported to be a characteristic of JET ICRF-only H-modes. More recent experiments, as illustrated next, showed that edge co-rotation is also observed.

More recent angular frequency measurements in another pulse with $\beta_N \sim 1.3$ are shown in figures 5 and 6. This pulse is from 2009 experiments which compared type I ELMy H-mode plasmas with dominant NBI to plasmas with dominant ICRF [24], with up to 9 MW of coupled ICRF power. The H-mode was achieved during a pre-heating NBI phase, with NBI later substituted by pure ICRF heating (except for the NBI blips for diagnostic purposes). The bottom traces show the $C^{+6}$ angular frequency measured during three NBI blips, close to the centre of the plasma (R=3.1 m) and close to the edge (R=3.8 m). The rotation measured at the first blip was affected by the NBI pre-heating phase and is therefore omitted. Only the measurements at the beginning of the second and third blips have been taken into account for the rotation measurements in presence of ICRF. The measured values both in the centre and edge are quite low, $|\omega_\phi| \leq 2 \text{ krad/s}$. The radial angular frequency profile, obtained at the beginning of the 2nd blip, is plotted in figure 6. For comparison, the profile from a L-mode plasma with lower ICRF power is plotted in the same figure. There is no significant difference between intrinsic rotation frequencies measured in L-mode and H-mode. Also shown in the figure are $\omega_\phi$ profiles for plasmas with NBI heating. While with NBI the toroidal rotation increases with input power, in plasmas with only ICRF there is no clear correlation between toroidal rotation and ICRF power. Within the still small H-mode database, one can conclude that as in L-mode there is no correlation between rotation an $\beta_N$.

**II c – Rotation studies in H-modes with various levels for the magnetic field ripple**

JET has 32 toroidal field coils and, therefore, a very low ripple level. These 32 coils are electrically grouped in two sets of 16 coils, that can be independently powered. The toroidal magnetic field ripple can be increased in JET by reducing the current in one of the coil sets, thus effectively reducing the current carried in every second magnetic field coil. The ripple is largest in the outboard of the plasma where it is closest to the toroidal magnetic field coils. The ripple values quoted in this paper are taken at R=3.80m, z=0 m, which is close to the maximum value. In standard operation with 32 coils $\delta_{TF}$ =0.08%, but in the experiments reported here this was increased up to $\delta_{TF}$ =1.5%.

The toroidal field ripple can induce high heat fluxes to plasma facing components caused by losses of fast ICRF accelerated ions [26]. Thus the ripple experiments were restricted to modest ICRF powers, less than 4 MW, and mostly to H fundamental cyclotron resonances near the plasma centre, or on the high field side of the plasma. The ion losses also induce a counter current torque that was shown to have significant impact on the rotation profiles of discharges with a large external torque and heating supplied by NBI [27]. Similarly, in pure ICRF heated discharges the ripple induced ion losses are expected to produce a counter rotation. This was confirmed experimentally as it was observed that, as the ripple in the toroidal field increased, counter-rotation increased in both the edge and the core of the plasma [1], without having a significant effect on other bulk plasma profiles. It should be pointed that TF ripple also affected the rotation in Ohmic plasmas [1], with a very low fast particle content, and therefore, the effect of the TF ripple on the intrinsic rotation cannot entirely be explained by fast ion losses alone.

In spite of the restricted amount of ICRF power, H-mode plasmas were achieved in experiments with plasma current, $I_p$=1.5 MA. A reference low ripple case is shown in figure 7. The low ICRF power was not enough to sustain a type I ELM regime for very long, thus leading to a second H-mode phase with type III ELMs. For ripple values $\delta_{TF} \geq 1\%$ H-modes with the whole plasma column counter rotating were observed (figures 8 and 9). Core counter-rotation was observed to be larger in the phases with type III ELMs than with type I ELMs. This difference in toroidal rotation (which is also observed at low ripple) is not understood; it is not due to MHD effects and, it is not clear if this is a pedestal or a density effect.

## III - Comparison of JET rotation data with the multi-machine rotation scaling

In ref. [2] intrinsic rotation scalings were derived from data from six machines (Alcator C-mod, DIII-D, JET, JT-60 Tore-Supra and TCV). These data originated from a large variety of plasma conditions, heating techniques and machine sizes. It includes data from devices with very different toroidal magnetic field ripple values, ranging from the low values in JET with $\delta_{TF}$ =0.08% to Tore-Supra with $\delta_{TF}$ =7% [28]. Radial velocity profile measurements were not available for all machines. Thus the data from different machines was taken from different radial positions, e.g. from CXS measurements in the centre for Alcator C-Mod and Tore-Supra and at mid-radius for JET. In DIII-D where CXRS profile data (using NBI blips) was

available, a radius close to the edge (where a peak in co-rotation is observed in discharges with ECRH on-axis deposition [29]) was chosen. JET rotation profiles are not flat and given the large range of core rotation values observed it is not obvious what radius should be chosen for comparison with the other machines. In the following plots JET data at two normalised radial positions are shown, $\rho$ ~0.1 and $\rho$ ~0.8, except for the JET pulses prior to the year 2000, which appear in the original plot of reference [2], where only data for $\rho$~0.39 were available ($\rho$=0.35 was actually used in ref. [2]).

The multi-machine scalings of reference [2] suggest that both $M_A$ and $\Delta V_\phi$ increase with the plasma parameter $\beta$ and decrease with the plasma current. In figure 10, JET H-mode data not previously included in the multi-machine database of [2] are plotted in the diagram of $M_A$ versus $\beta_N$ (figure 7 of reference [2]). This plot shows the range of data used in ref. [2]'s scaling for $M_A$ and, the now available range of JET data. Since the original plot mixes devices with different magnetic field ripple values, the new JET data plotted here includes experiments with low and high values of the magnetic field ripple ($\delta$=1%-1.5%). When compared with measurements from other machines intrinsic co-rotation frequencies in the newly added JET ELMy plasmas are quite low, typically less than 10 krad/s (~30 km/s). In some cases the observed rotation, either in the core or in the edge, is in the counter-direction, even for the low ripple case. While in other machines $M_A$ increases with $\beta_N$, JET intrinsic rotation show no clear dependence on $\beta_N$.

Values of $M_A$ measured in JET, for pulses with the usual low ripple, are compared with ref. [2]'s $M_A$-scaling: $M_A= 0.65\beta^{1.4}q_*^{2.3}$, where $q_*=2\pi\kappa a^2B/\mu_0RI_p$ in figures 11a and 11b. JET ICRF rotation in ELMy regimes is below Rice's $M_A$-scaling law. With the standard low ripple configuration, JET plasmas with large ICRF heating power and normalized beta, $\beta_N \approx 1.3$, have a very small co-current rotation, in clear contradiction with ref. [2]'s $M_A$-scaling law that would in most cases extrapolate to roughly 10 times higher Alfven-Mach numbers for the same $\beta_N$ value. Cases with either core or edge counter-rotation can evidently not fit the scaling where all the data included were co-rotating. However, since the direction of the rotation may not be important for MHD stabilization, it makes sense to compare the highest $M_A$ values obtained experimentally independently of the direction of rotation. Thus the $M_A$ absolute values from a few counter-rotation cases have been included in figure 10. These are also lower than ref. [2]'s 's $M_A$-scaling. Fig. 11b shows the JET data superimposed on figure 8 of ref. [2]. Shown in this figure are the $M_A$ values for two possible ITER operational regimes,

used for rotation predictions for ITER. Clearly with the new JET data, a different $M_A$ scaling would have been obtained and lower ITER rotation values would have been predicted.

The other scaling presented in reference [2] is for the difference of rotation velocities observed in enhanced regimes and L-mode, $\Delta V_\phi = V_\phi^H - V_\phi^L$. The enhanced regimes included H-modes, as it is the case of JET, and plasmas with improved performance as in Tore-Supra. Only enhanced regimes with rotation changes in the co-direction, i. e. $\Delta V_\phi > 0$ were considered. From the best fitting for 6 machines it was obtained that $\Delta V_\phi \propto B_0^{1.1} \Delta < p >^{1.0} I_p^{-1.9} R^{2.2}$ (where <p> is the average pressure). In figure 12, $\Delta V_\phi$ observations in low ripple JET H-mode plasmas are added to figure 1 of ref. [2], from where we kept only Alcator C-Mod and DIII_D, as our intention is to compare JET with other H-mode plasmas. JET $\Delta V_\phi$ values are lower than observed in other machines, since in JET there is no significant difference between intrinsic rotation frequencies measured in L-mode and H-mode. Often rotation frequencies in H-mode are lower than in L-mode giving negative $\Delta V_\phi$ values, even when $V_\phi$ is positive. Near the edge, at r/a~0.8, $\Delta V_\phi$ values are negative and therefore do not fit ref. [2]'s scaling for $\Delta V_\phi$, which is a scaling for plasmas where co-rotation increases after the L-H transition. A comparison of velocity rotation changes in the core of JET plasmas, with H-mode plasmas from Alcator C-Mod and DIII-D suggest a size scaling with $\Delta V_\phi \sim R^{-a}$, with a>2. Ref. [2]'s scaling for $\Delta V_\phi$ on the other-hand suggests that $\Delta V_\phi$ should increase with R.

As the ripple in the toroidal magnetic field increased, both the edge and the core of JET plasmas counter rotated. Core counter-rotation was observed to be larger in phases with type III ELMs, but even type I-ELMy plasmas with normalized $\beta_N \approx 1$ were counter-rotating. These results do not fit the multi-machine scalings which were derived for co-rotating plasmas. Assuming that the direction of rotation is not relevant, then one should note that plasmas with type III ELMs achieved the highest counter-rotation ,with values in the core of up to 20 krad/s (~60 km/s) for ripple ~1.5%. Counter-rotation could be further increased by moving the ICRF resonance position to the low-field side [1] although for the safety of the wall facing components this may be undesirable.

## IV - Discussion and Conclusions

This paper summarized the measurements of angular velocity in JET H-mode plasmas collected over several years. It included data from JET in its standard low toroidal magnetic ripple configuration ($\delta_{TF}$ =0.08%), and from a special experimental campaign when the ripple was increased (up to $\delta_{TF}$ =1.5 %). The JET H-mode data, and in particular data from ELMy H-modes not previously included in a multi-machine database, was compared with the multi-machine rotation scaling [2] for the Alfven-Mach number and the scaling for the velocity change from L-mode into H-mode. These two scalings, derived for co-rotating plasmas do not reproduce well the JET data.

With the standard low ripple value $\delta_{TF}$ =0.08%, JET plasmas with large ICRF heating power and normalized $\beta_N \approx 1.3$, have a very small co-current rotation. The multi-machine rotation scaling [2] would in most cases extrapolate to roughly 10 times higher Alfven-Mach number for the same $\beta_N$ value. Whilst the edge of JET L-mode plasmas is co-rotating, in ELMy H-modes both edge co- and counter-rotation has been observed. JET rotation in minority heated ICRF plasmas shows no dependence on ICRF power or on $\beta_N$. No significant difference between H-mode and L-mode rotation is observed, except that the H-mode velocities near the edge are in general slightly lower than in L-modes. The JET data shows different scalings for the edge and core rotation, indicating that different physics is determining the rotation at the edge and core.

The reason why high co-current rotation has not been observed in recent JET H-modes with ICRF heating is not yet understood. The highest co-rotation was observed in ELM-free, low density plasmas with the Mark-I divertor [11]. Subsequent rotation measurements, with higher $P_{ICRF}$ and higher $\beta_N$ values, reported in [12] and here, were obtained in ELMy plasmas with more closed divertors. It is not known if differences in the observed rotation in the old and the new experiments are due to differences in density, pedestal or scrape-off layer physics. Recent papers have been focusing on the relationship between edge plasma parameters and the intrinsic rotation scaling [30-31]. In Alcator C-Mod , $\Delta V_\phi$ in the plasma centre was found to correlate with the temperature gradient near the edge. Electron temperature and temperature gradients are higher in the JET ELM-free pulse (shown in fig. 2) than in the newer ELMy pulses (figs.3-5), that may lead to a higher pedestal and core rotation. Pedestal parameters however cannot easily predict JET observations where in many cases central and edge regions rotate in the opposite direction [17, 32].

The low co-rotation observed in the core of JET H-modes with ICRF-only may in some cases be caused by MHD modes. For instance, in the pulse shown in figure 5, fishbones are observed. In one of the high ripple cases, increased counter-rotation was observed when core-TAE modes were present. Both fishbones and core TAEs, via a redistribution of ICRF accelerated trapped ions could give rise to a counter-current torque. Low co-rotation in the edge, on the other hand, might be caused by ELMs. Separation between effects driven by ICRF from those caused by either core or edge MHD instabilities is not easy since with CXRS at JET only snap shots of rotation profiles are available.

The effect of ELMs on toroidal rotation has been studied in JET plasmas with NBI heating [33]. With NBI, a large reduction in angular frequency at the plasma edge is observed to penetrate into the plasma up to r/a ~ 0.65 during large type-I ELMs. In the NBI pulses, the time averaged angular frequency is lowered near the top of the pedestal with increasing ELM frequency. Substituting NBI by ICRF heating does not change the pedestal properties and the ELM frequency [24]. ELMs can affect the rotation of ICRF dominated plasmas (see figure 4). However the rotation database for plasmas with pure-ICRF is at the moment too small thus it is not possible to quantity the effect on toroidal momentum as a function of ELM frequency. In figure 5, the low co-rotating angular frequency is measured at the edge with an ELM frequency of 40 Hz. In figure 3, the counter rotating edge is observed when the ELM frequency is 100 Hz. However just before this measurement is made, a sawtooth crash is observed, making it difficult to pinpoint which event may be responsible for driving counter-rotation at the edge. If ELMs can drive counter-rotation then this could be through the loss of ICRF fast-ions. In NBI heated plasmas with increased toroidal field ripple and counter rotating edge, ELMs did not increase the counter rotation, rather the opposite was observed as each ELM would reduce the counter-rotation to zero [27]. Thus the ELM does not seem to cause a loss of fast-NBI ions that is significant for driving a counter-torque. It is not clear if the same would apply for losses of fast ICRF ions. The small dispersion in the DIII-D data show in figures 10-12, which mixes Ohmic H-modes as well as ECRF H-modes with no distinction between measurements taken during ELM-free and ELMy phases [29], appear to indicate that ELMs in DIII-D plasmas do not have a significant effect on intrinsic rotation. However since the heating mechanism is different, it is still leaves open the question of how ELMs and their interaction with fast ion losses may influence rotation in plasmas with no momentum input.

The rotation scaling of reference [2] included data from machines with a wide range of magnetic field ripple from low values of <0.1% as in JET to 7% in Tore Supra. The Tore

Supra discharges with the co-rotating centre that were included in the scaling appeared to suggest that ripple could be neglected. In ICRF heated Tore Supra discharges, both counter and co-current acceleration of the central plasma has been observed when the power is switched on [28, 34]. However, the majority of the ICRF heated Tore Supra discharges with full plasma size, and hence standard large ripple level, appear to be counter rotating [35]. In the ones, included in the multi-machine scaling of ref. [2], where a co-current acceleration has been reported, a key factor seems to have been a low fraction of fast particle losses combined with a significant ion heating fraction [28, 34]. It is worth stressing here that Tore Supra data appearing in the multi-machine scaling are from non wavelength-calibrated XCS measurements [36]. The data set indicates that the changes observed in rotation from a low to a higher confinement plasma phases (namely from Ohmic to ICRH phases) are in the co-current direction. Whether the velocity itself is co- or counter-rotating is not possible to determine, therefore one should be cautious when considering those data in the $M_A$ scaling together with co-rotating plasmas.

JET experiments at different ripple values showed that ripple has a significant effect on the plasma rotation observed in the absence of external momentum sources [1]. In JET as the ripple in the toroidal magnetic field increased, both the edge and the core of JET H-mode plasmas, with dominant ICRF heating, counter rotated. Core counter-rotation was observed to be larger in phases with type III ELMs, but even type I-ELM plasmas with normalized $\beta \approx 1$ were counter-rotating. These results do not fit either of the multi-machine intrinsic rotation scalings of [2] which are for co-rotating plasmas. The JET results from magnetic field ripple experiments shows that measurements with high ripple should not be included in a scaling where machines with low ripple are also included. The JET experiments which were done at ITER-relevant ripple values [37], show that at $\delta_{TF} = 0.5\%$ JET H-mode plasmas with ICRF heating are hardly rotating [1], while at $\delta_{TF} = 1\%$, counter-rotating H-modes were observed. These results suggest that ripple will affect rotation in ITER, of course it will depend on the value of ripple that ITER will eventually have and, it should be taken into account in extrapolation from present data.

A multi-machine scaling for intrinsic rotation was found in ref [2]. In this paper we showed that plasmas with intrinsic rotation can be found at JET that do not follow the scaling. It is likely that the entries in the database, on which the scaling was based, have intrinsic rotation that is governed by the same physics. At JET however, other physics mechanisms may play a dominant role, such that these deviate from the scaling. These should be taken into

consideration when extrapolating to ITER. Experimentally several factors have been found to play a role in determining intrinsic rotation in plasmas with ICRF heating: magnetic field ripple, core and edge MHD modes, heating details as for instance the location of ICRH resonance, plasma current and H-mode scenario. The large variation in the core velocities indicate a complex situation where rotation depends strongly on the transport properties of the plasma, heating details, fast particles and even MHD activity. For comparison of different machines the way forward should be similarity experiments with strict conditions.

In conclusion, JET results, either with or without taking into account the effect of toroidal magnetic field ripple, suggest that ITER intrinsic rotation may well be substantially less than what was predicted by multi-machine rotation scaling of ref. [2].

**Acknowledgments**

This work was supported by EURATOM and carried out within the frameworks of the European Fusion Development Agreement. It received financial support from Fundação para a Ciencia e Tecnologia (FCT), Portugal. The views and opinions expressed herein do not necessarily reflect those of the European Commission. M. F. F. Nave is grateful to A. Schekochilin and other members of the Plasma Group at the Rudolf Peierls Centre for Theoretical Physics, Oxford University for useful discussions and for their hospitality. The authors are grateful to the Nuclear Fusion Journal and for John Rice for giving their permission to add new measurement points in some of the original plots showing the Rice scaling. We are grateful to J. Rice, J. de Grassie and C. Fenzi for useful discussions.

**References**

[1] M.F.F.Nave et al., PRL **105**, 105005 (2010)

[2] J.E.Rice et al, Nuclear Fusion **47**, 1618 (2007)

[3] M.N.Rosenbluth and F.L.Hinton, Nuclear Fusion **36**, 55 (1996)

[4] R. Budny, Nuc Fusion **49**, 085008 (2009)

[5] P.C. de Vries, et al. Nucl. Fusion **48** (2008) 065006

[6] T. Tala, et al., Plasma Physics and Controlled Fusion 49, B291 (2007).

[7] T. Tala et al., Phys. Rev. Lett. 102, 075001 (2009).

[8] W.M. Solomon et al., Nuclear Fusion 49, 085005 (2009)

[9] M. Yoshida et al., Nucl. Fusion 47, 856 (2007).

[10] A.G. Peeters et al., "Overview of toroidal momentum transport", submitted to Nucl. Fusion.

[11] L-G Eriksson, E. Righi and K-D Zastrow, Plasma Phys. Control Fus. **39**, 27 (1997)

[12] J.-M. Noterdaeme et al. NF **43**, 274 (2003)

[13] A. Kaye et al, Fusion Engineering and Design **24** (1994) 1-21]

[14] Durodie F et al 2005 Fusion Eng. and Design 74 223

[15] M.-L. Mayoral et al., 36th European Physical Society Conference on Plasma Physics Sofia, Bulgaria, June 29 - July 3, 2009 ECA Vol.**33E**, O-4.048 (2009)]

[16] F. Durodié et al., Proc. of the 23rd IAEA FEC2010, Daejeon, Korean, EXC/P7-04

[17] L.-G. Eriksson et al., Plasma Phys. Control. Fusion **51** (2009) 044008

[18] Y. Lin et al, Physics of Plasmas 16 056102 (2009)

[19] Y. Lin et al. 37th EPS Conference on Plasma Physics, Dublin (2010), paper P5.164

also in Y. Lin et al, PPCF this issue (2011)
[20] F. Bombarda et al, Phys. Rev. **A 37**, 504(1988)
[21] C. R. Negus et al., Rev. Sci. Instrum. **77**, 10F102 (2006)
[22] C. Giroud et al, Review of Scientific Instruments **79**, 10F525 (2008)
[23] Eriksson et al, Plasma Phys. and Contr. Fusion. Vol. **34**. No. 5. pp 863 to 871. l992
[24] R. Sartori et al, Proc. of the 23rd IAEA FEC2010, Daejeon, Korea, EXC/P8-12
see also, T.W. Versloot et al., To be submitted to N.F. (2010)
[25] L.D. Horton et al 1999 Nucl. Fusion **39** 1
[26] T. Johnson et al., 10th IAEA TM Energetic Particles in Mag. Conf. Systems, Kloster Seeon, Germany (2007)
[27] P. de Vries et al, N.F. **48**, 35007 (2008)
[28] L.-G. Eriksson, G.T. Hoang and V. Bergeaud, Nuclear Fusion **41**, 91 (2001).
[29] J de Grassie et al., Physics of Plasmas **14**, , 056115 (2007)
[30] W. Solomon et al., NF v51 073010 (2011)
[31] J.E. Rice et al. , PRL v106 215001 (2011)].
[32] F. Parra etal, submited to PRL (2011)
[33] T.W. Versloot, et al., Plasma Phys. Control. Fusion 51 (2010) 045014
[34]. Assas S. et al 2003 Toroidal plasma rotation in ICRF heated Tore Supra discharges 30th EPS Conf. on Plasma Physics and Controlled Fusion (St Petersburg)
[35]. C. Fenzi et al, NF 51 (2011) 103038))
[36] C. Fezzi, private communication (2011)
[37] Saibene G. et al., in Proc. 22nd IAEA Fusion Energy Conf., EX/2-1 (Geneva, 2008)

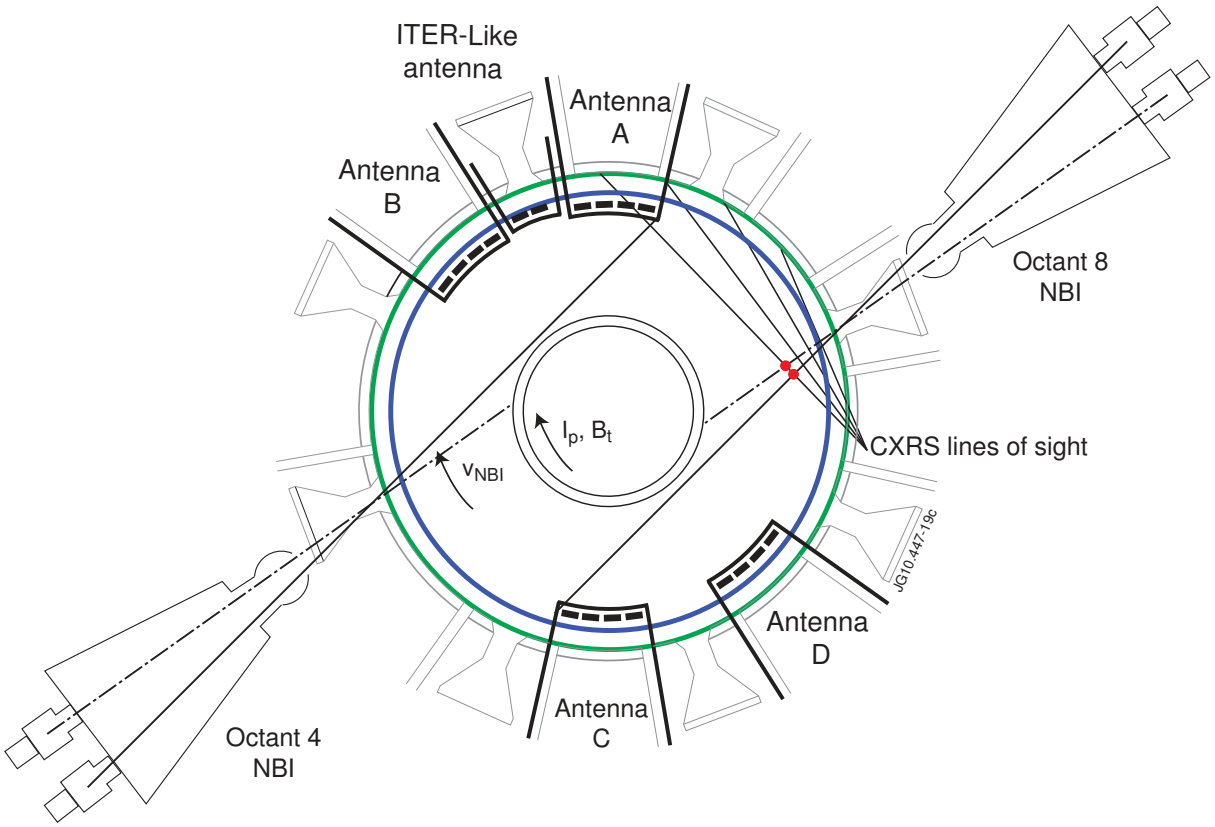


Figure 1. Schematic view from the top of JET showing the positions of the four A2 ICRF antennae and the ITER-like ICRF antenna. Also shown are the two NBI injectors and NBI lines which are parallel (solid lines) and near perpendicular (dotted lines) and, the CXRS lines of sight. The three CXRS emission layers which contribute to the measured spectra are indicated as: the cold non-rotating SOL in green, the passive warm and rotating slowly layer in blue and the active hot and strongly rotating region which is shown by red dots in the intersection of beam lines and CXRS lines of sight. Also indicated in the figure are the usual directions of the toroidal field $B_T$, the plasma current $I_p$ and the usual direction of the rotation induced by NBI, $v_{NBI}$ (which in the case of low ripple is in the co-current direction).

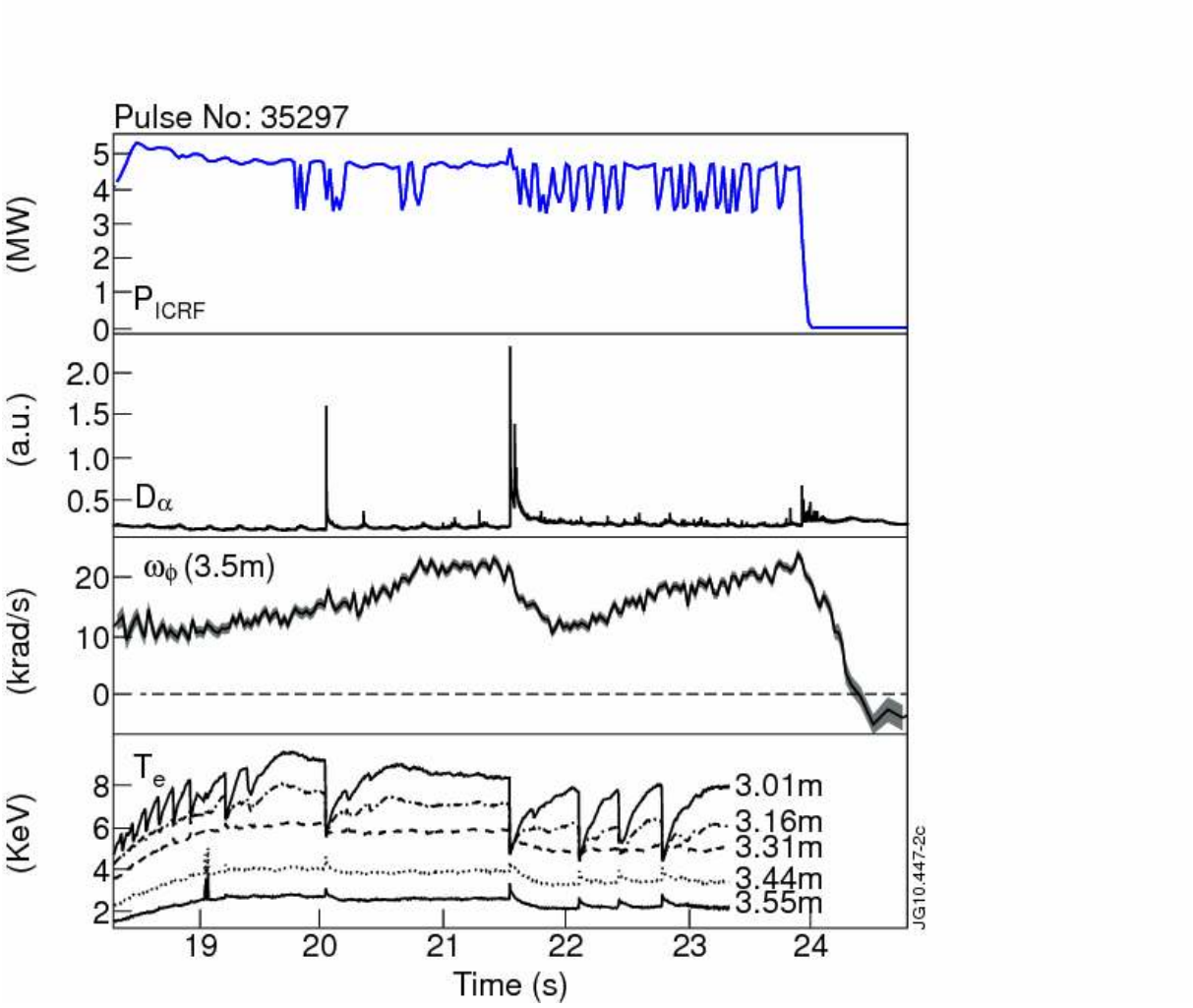


Figure 2. Pulse with $P_{ICRF}$~4.5 MW, $R_{res}$=2.93 m, $R_0$=2.97 m, $I_p$=3MA, $B_T$=3T, maximum $\beta_N$~0.6 showing the largest co-rotation observed in a JET H-mode plasma with ICRF-only. The plots show: (a) $P_{ICRF}$, (b) $D_\alpha$ (where small regular fluctuations are caused by divertor target sweeping), (c) $Ni^{+26}$ rotation measured by XCS at R=3.5 m (r/a=0.39), shaded area shows measured uncertainty and, (c) electron temperature traces at different radii. The L-H transition is at t ~ 18.9 s.

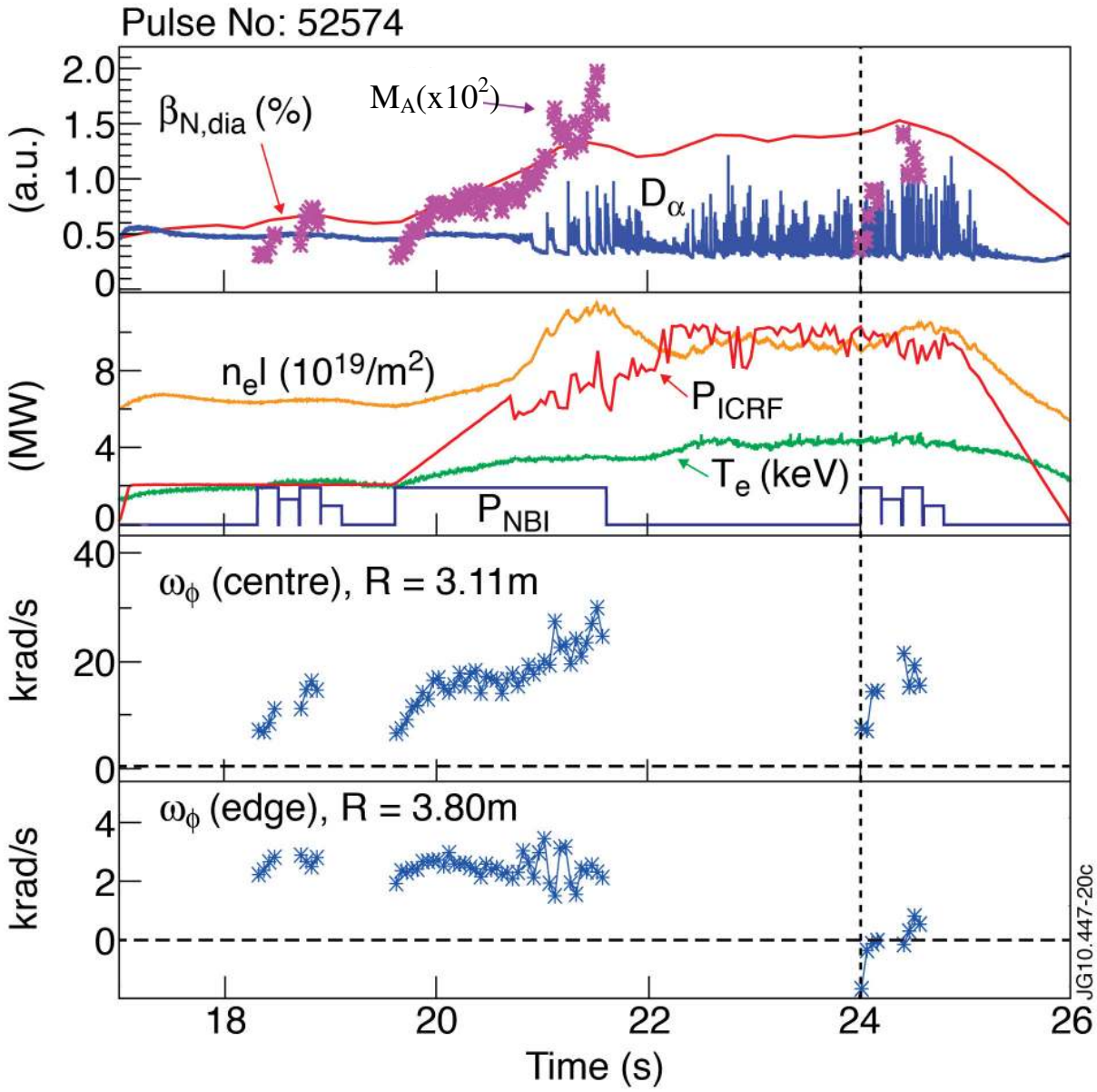


Figure 3 - Pulse with $P_{ICRI}$ ramped from 2 to 10 MW, $R_{res}$=2.7 m, $R_0$=2.98 m, $I_p$=2 MA, $B_T$=2.45 T, maximum $\beta_N$~1.3. The plots show: (a) $D_\alpha$, EFIT Diamagnetic $\beta_N$ value and $M_A$(x100) near the centre (R=3.11 m), (b) $P_{ICRI}$ , $P_{NBI}$ , central $T_e$, central integrated density $n_e l$, (c) $C^{+6}$ rotation angular frequency measured near the centre (R= 3.11 m) and, (d) near the edge (R= 3.8 m). The vertical line indicates the time chosen for the data shown later in plots 10-12.

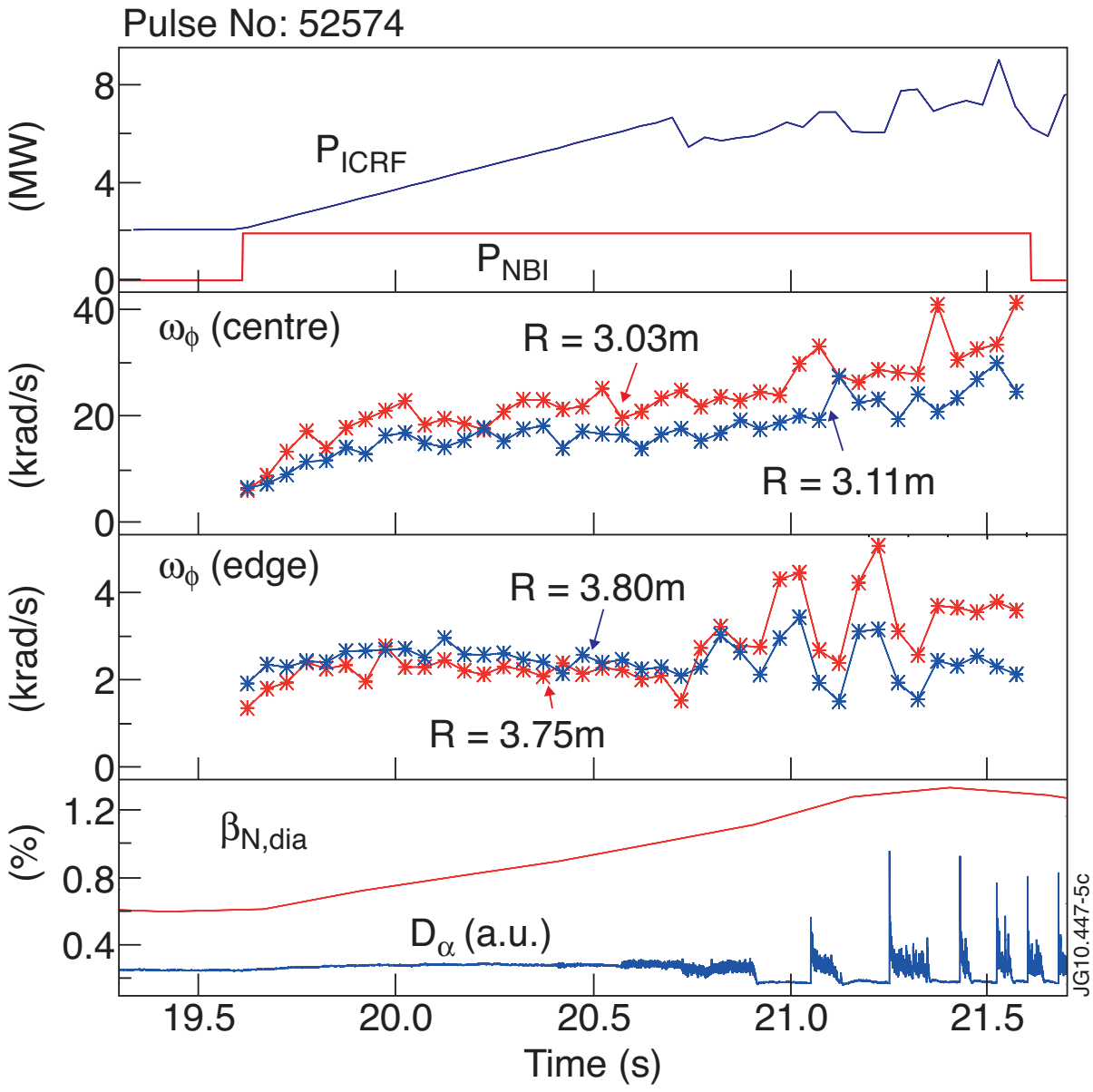


Figure 4 - Close up of figure 3, showing L-H transition that occurs during a continuous phase of NBI heating, when ICRF power is ramped up. Plots show; (a) $P_{ICRF}$ and $P_{NBI}$, (b) $C^{+6}$ angular frequency measurement at two central positions (3.05 m and 3.11 m) and (c) two positions near the edge (3.75m and 3.80 m), (d) $D_\alpha$ and diamagnetic $\beta_N$. The L-H transition occurred at t ~ 20.78 s. The edge $\omega_\phi$ increases in the H-mode but only during long ELM-free phases. It remains a level lower than observed in the ELM-free phase once regular ELMs start.

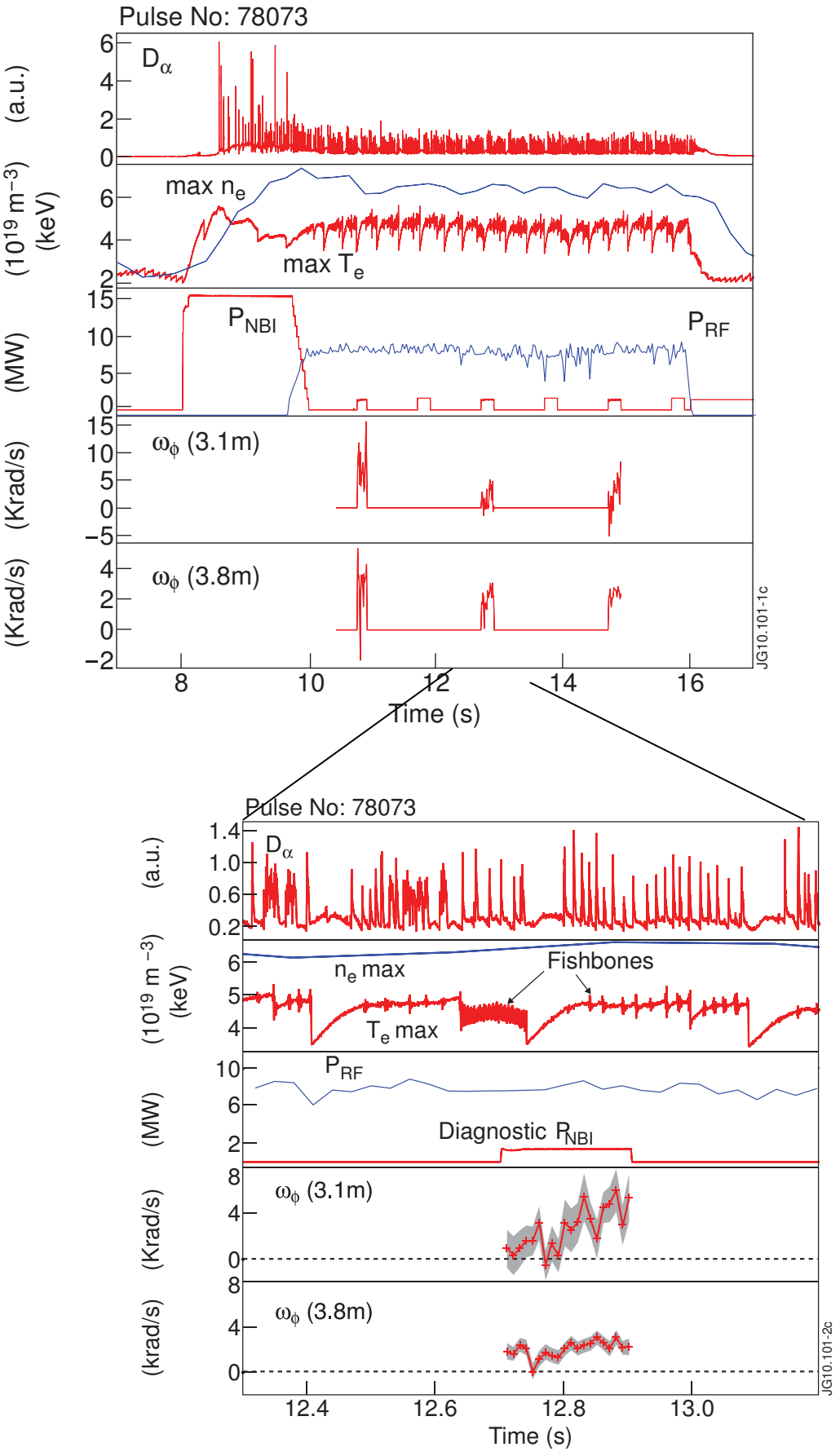
Pulse No: 78073
Dα
(a.u.)
max ne
max Te
(10^19 m^-3)
(keV)
PNBI
PRF
(MW)
ωφ (3.1m)
(Krad/s)
ωφ (3.8m)
(Krad/s)
JG10.101-1c
Time (s)
Pulse No: 78073
Dα
(a.u.)
ne max
Fishbones
Te max
(10^19 m^-3)
(keV)
PRF
Diagnostic PNBI
(MW)
ωφ (3.1m)
(Krad/s)
ωφ (3.8m)
(krad/s)
JG10.101-2c
Time (s)

Fig. 5 - H-mode with ICRF heating (except for NBI blips) with $P_{ICRF}$~9 MW, $R_{res}$=2.90 m, $R_0$=3.00 m , $I_p$=2.5 MA, $B_T$=2.6 T , $\beta_N$~1.3. The plots show the time evolution of : (a) $D_\alpha$, (b) maximum values of $n_e$ and $T_e$, (c) $P_{ICRF}$ and diagnostic $P_{NBI}$. (d) and (e) show respectively the charge exchange measurements of the $C^{+6}$ toroidal angular frequency in the centre (R=3.1 m) and close to the edge (R=3.8 m). The angular frequency profile measured at the beginning of blip n.2 is shown is figure 6.

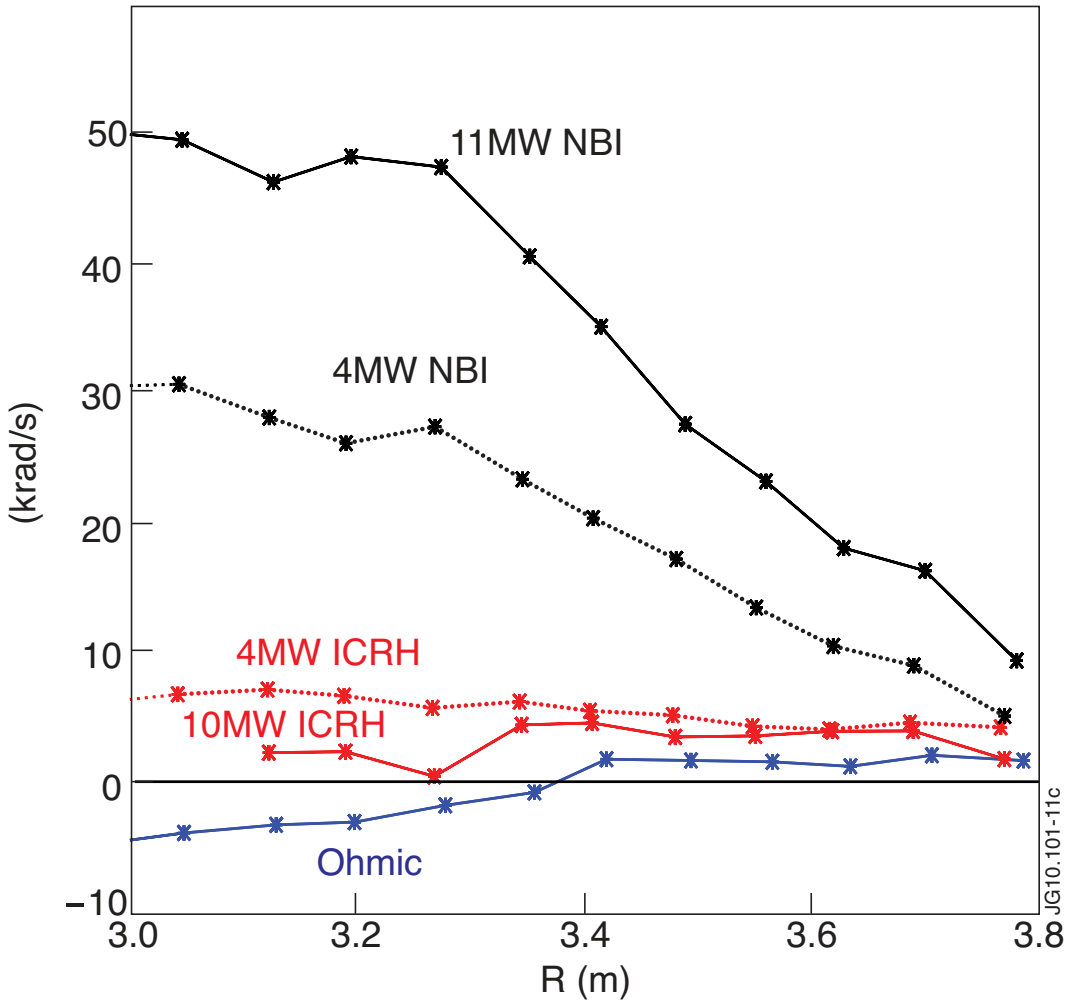


Fig. 6 - $C^{+6}$ toroidal angular frequency radial profiles measured for two ICRF heated plasmas: an H-mode with $P_{ICRF}$=10 MW (pulse from figure 5, second NBI blip) and a L-mode with $P_{ICRF}$=4 MW. NBI and Ohmic heated pulses for comparison.

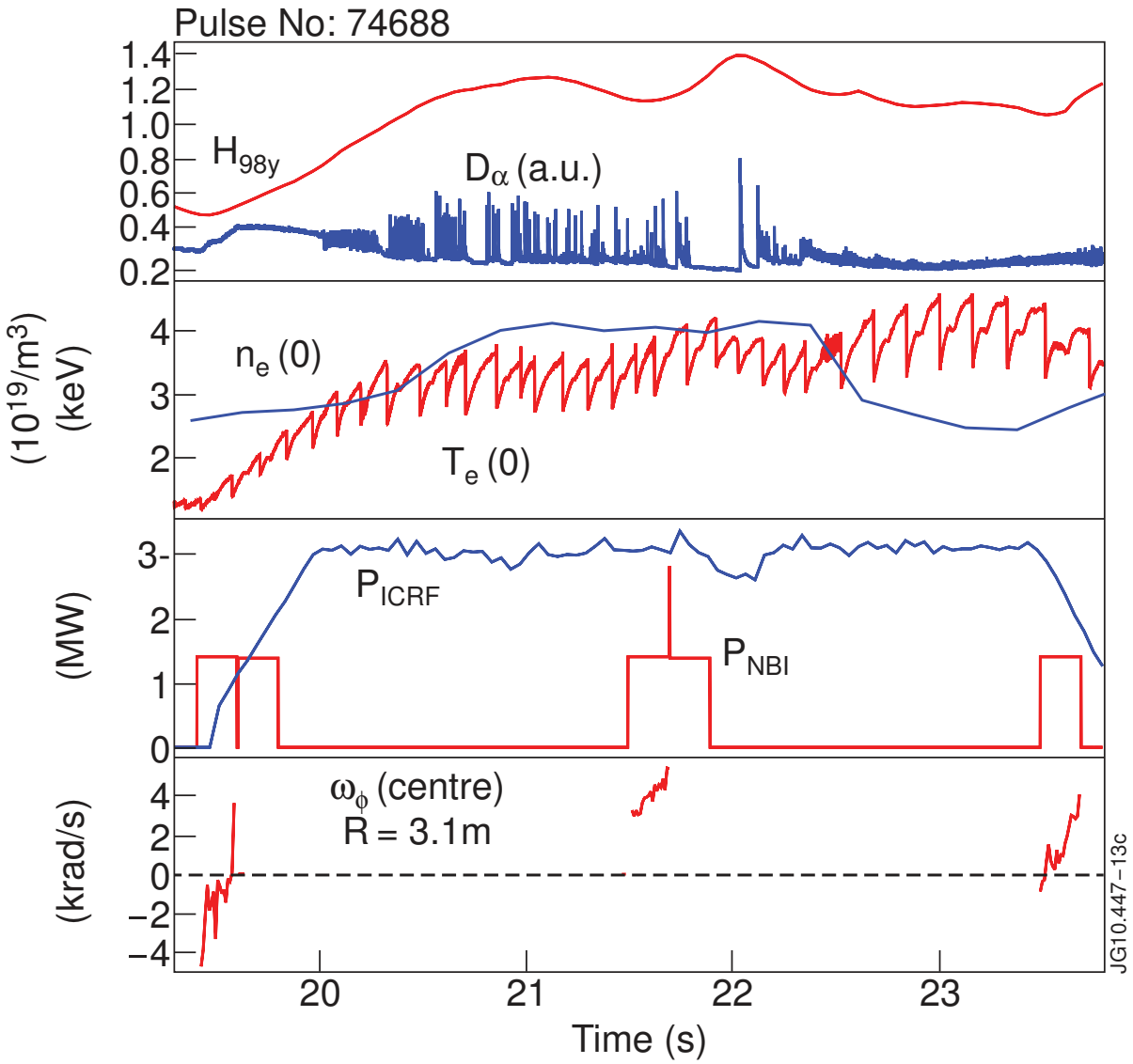


Figure 7 - Low ripple pulse ($\delta_{TF}$ =0.08%) used as reference for intrinsic rotation experiments with higher ripple at low plasma current. This pulse has $I_p$=1.5 MA, $<B_T>$=2.2 T, $P_{ICRF}$~3 MW. The plasma centre is at $R_0$=3.02 m, the ICRF resonance is slightly off-axis on the high-field side at $R_{res}$= 2.71 m . The plots show: (a) $D_\alpha$, H mode factor $H_{98y}$, (b) central electron temperature and electron density, (c) $P_{ICRI}$ , $P_{NBI}$, (d) $C^{+6}$ rotation angular frequency measured near the centre (R=3.1 m). Rotation profiles at the beginning of the 2nd NBI blip, when type I ELMs are observed and at the beginning of the 3rd NBI blip when type III ELMs are present, are shown in figure 8.

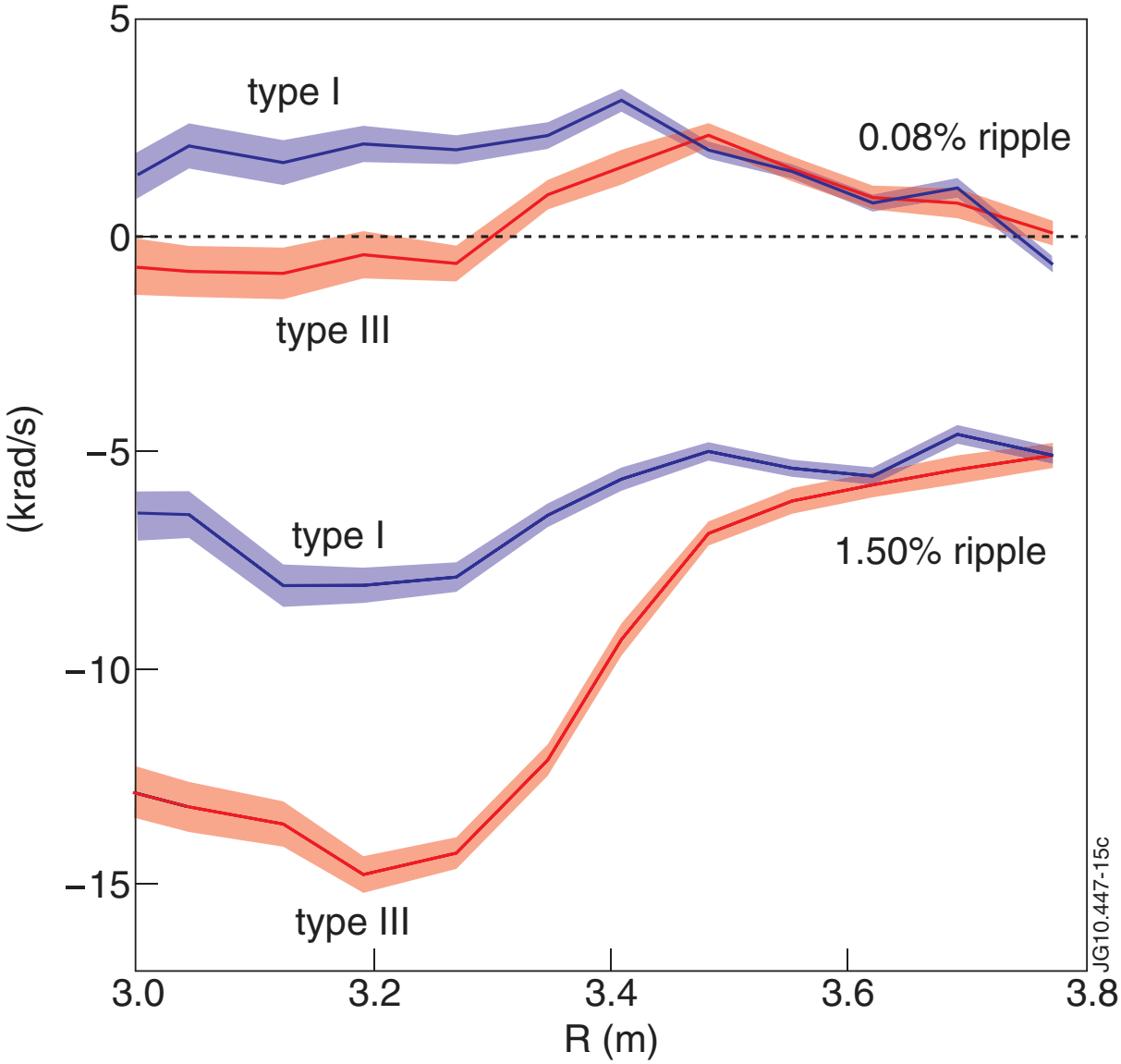


Fig.8 – Toroidal rotation angular frequency profiles for ICRF heated H-mode plasmas with $I_p$=1.5 MA, $<B_T>$=2.2 T, $P_{ICRF}$~3 MW for two ripple levels. Top: pulse # 74688 with $\delta_{TF}$ =.08% and $P_{ICRF}$=3.1 MW (shown in figure 8a); bottom: pulse # 74686 $\delta_{TF}$ =1.5% and $P_{ICRF}$= 2.9MW. The plasma centre is at $R_0$=3.02 m, the ICRF resonance is slightly off-axis on the high-field side at $R_{res}$= 2.71 m .

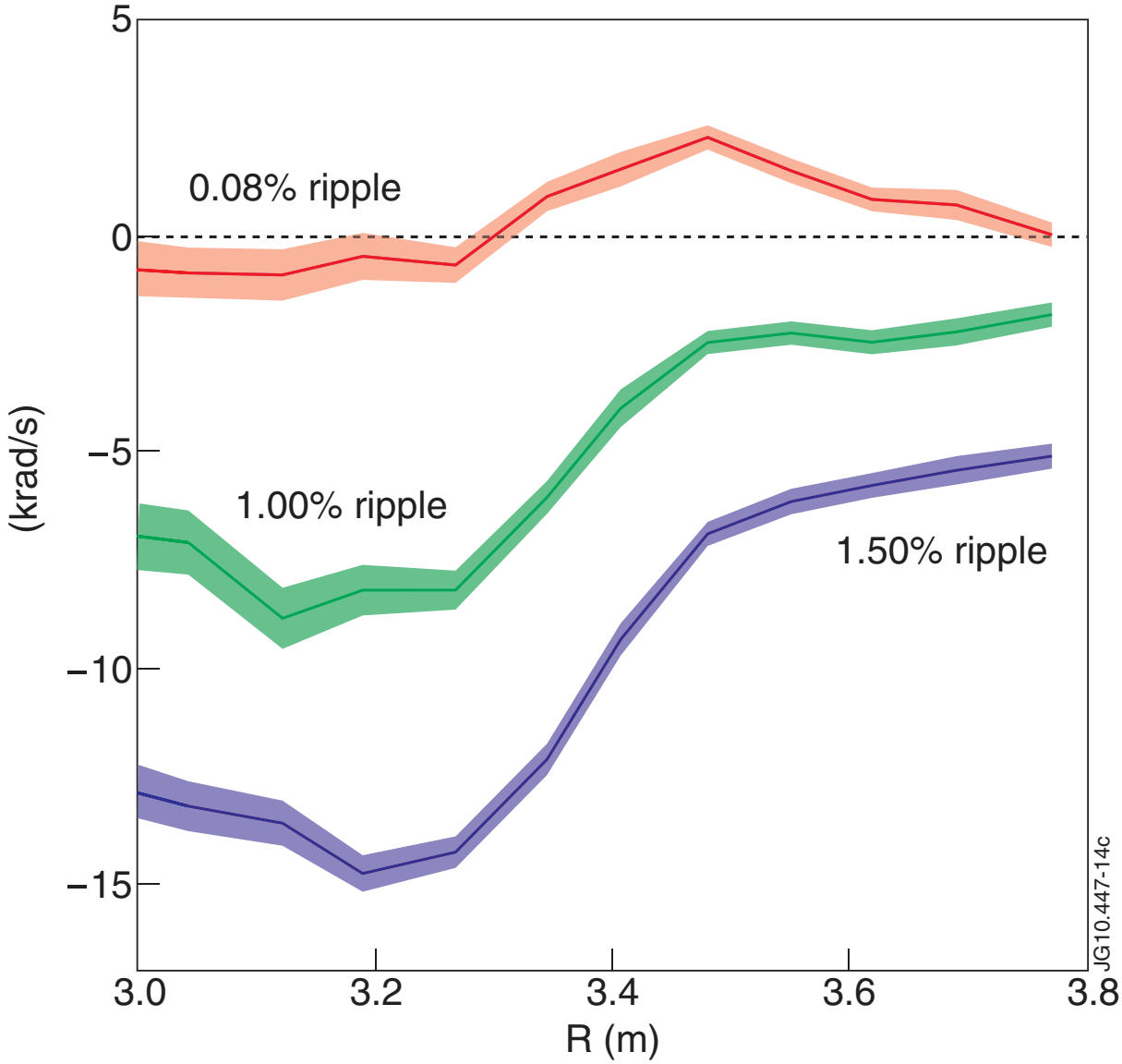


Figure 9 - Toroidal rotation angular frequency profiles measured during type III ELMy phases, at three ripple levels (pulse # 74688 with $\delta_{TF}$ =.08%, pulse # 74687 with $\delta_{TF}$ =1% and pulse # 74686 with $\delta_{TF}$ =1.5%), with $I_p$=1.5 MA, $\langle B_T \rangle$=2.2, $P_{ICRF}$~3 MW, the plasma centre at $R_0$=3.02 m, the ICRF H fundamental resonance slightly off-axis on the high-field side at $R_{res}$= 2.71 m .

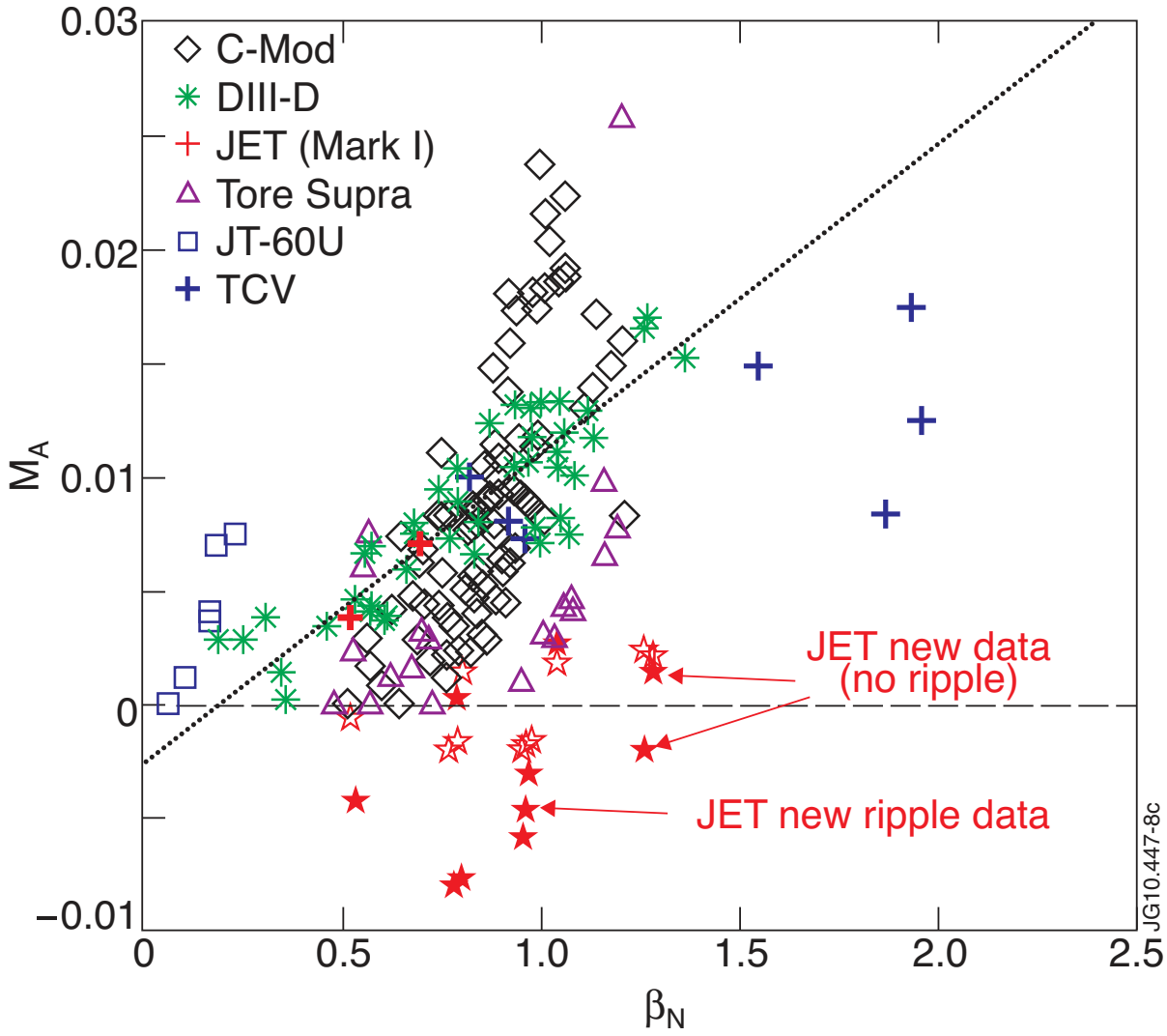


Figure 10 - Plot from Reference [2}, reproduced with permission from N.F. that shows the range of data in the multi-machine database, with new JET data added: open star symbols for edge values (r/a~0.8) and solid symbols for the core (r/a~0.1).

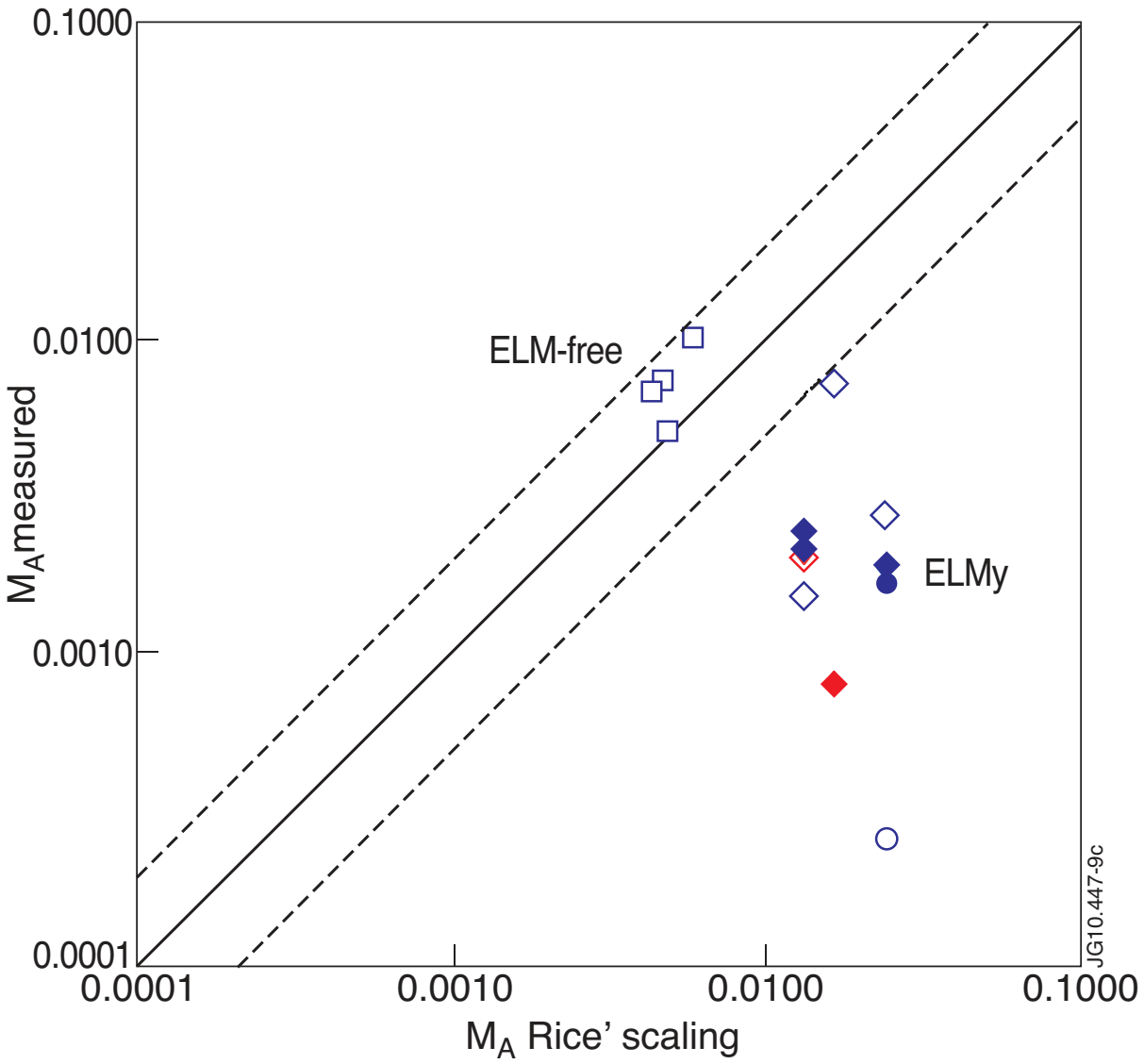


Figure 11a - JET measured $M_A$ H-mode plasmas with ICRF heating versus the Rice's $M_A$-scaling. Only data from experiments in the usual low ripple configuration are shown, indicated by the following symbols: squares for old ELM-free plasmas, kites for ELMy type-I plasmas, circles for ELMy type-III plasmas. Open symbols are measurements in the plasma core: r/a~0.1 for ELMy plasmas; r/a~0.39 for the old ELM-free plasmas (in ref. [2] r/a~0.35 was used ), while solid symbols are from the edge: r/a~0.8. Red are for counter-rotation, absolute value plotted, which strictly speaking doesn't fit the $M_A$ scaling which considered only co-rotating plasmas. The core measurements of the old ELM-free plasmas fit the Rice scaling within a factor of two (dotted lines show a factor of two variation). Data from ELMy regimes is lower than predicted by the scaling.

.

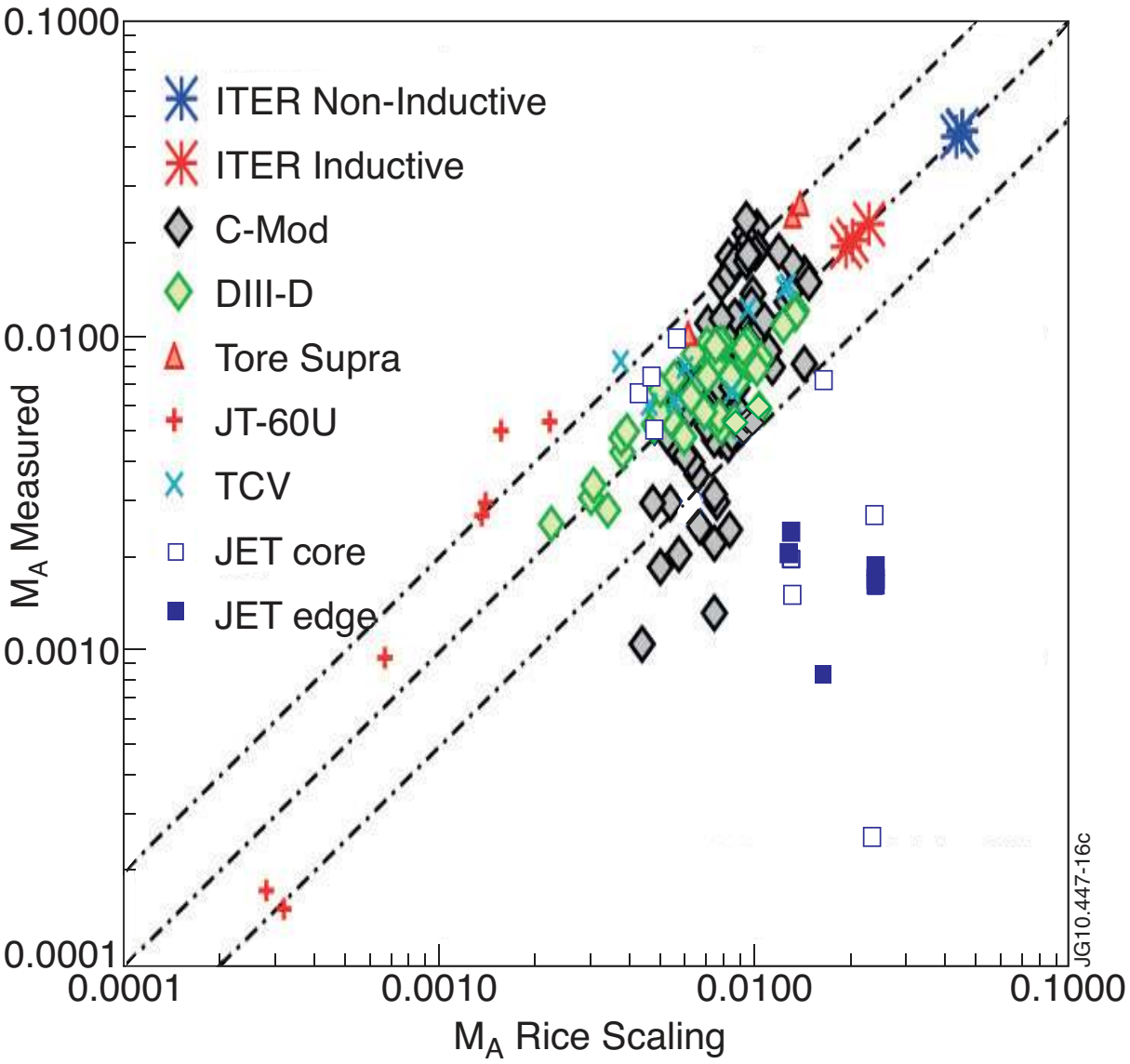


Figure 11b - Same JET data as in figure11a superimposed on figure 8 from Ref. [2] (reproduced with permission from N.F.).

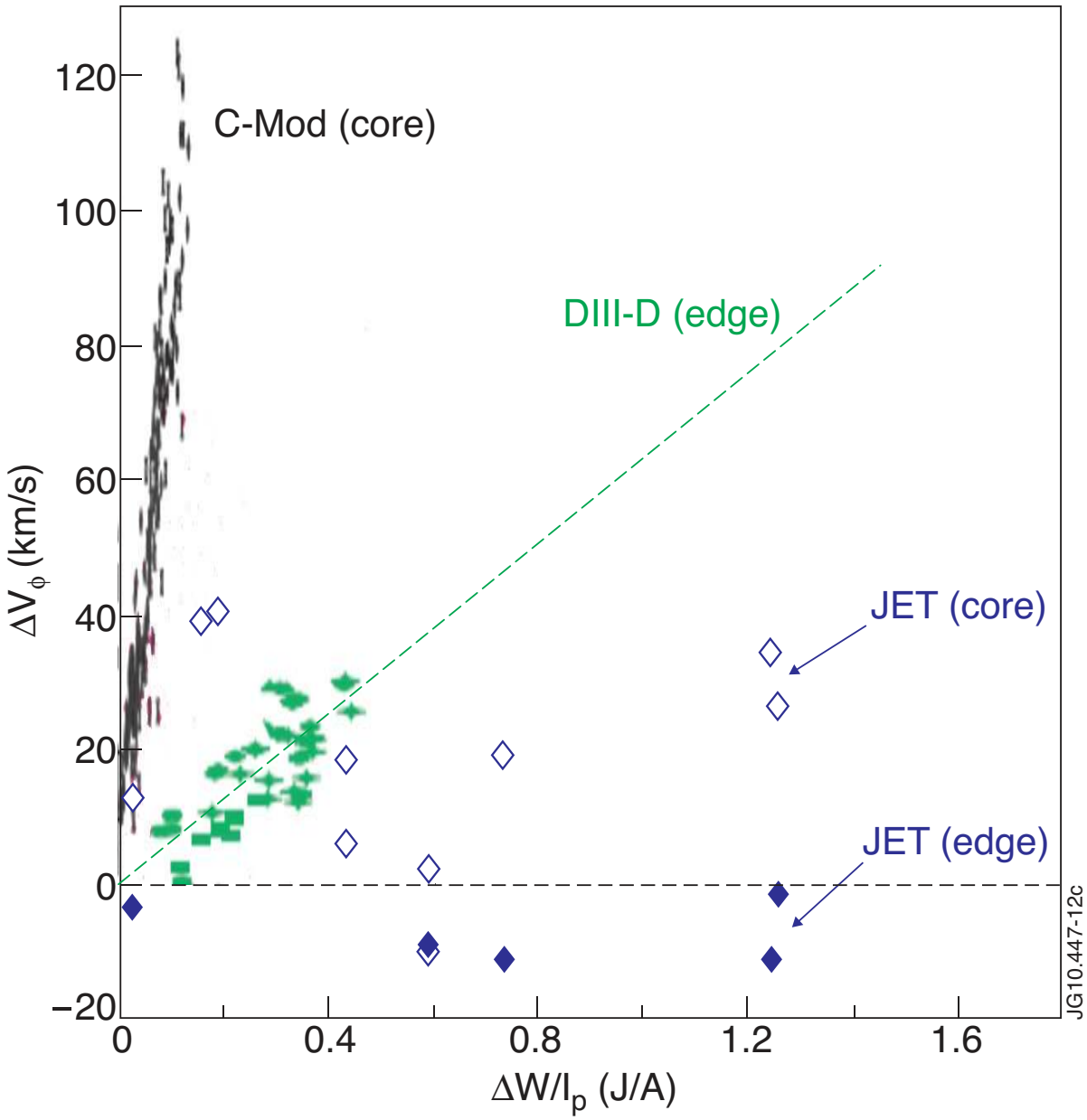


Figure 12 - JET measurements of $\Delta V_\phi = V_\phi^{\text{H-mode}} - V_\phi^{\text{L-mode}}$ versus the change in plasma stored energy, W, divided by $I_p$, together with H-mode data from Alcator C-mod (r/a~0.1) and DIII-D (r/a~0.8) taken from figure 1 of ref. [2] (reproduced with permission from N.F..). Only JET data from experiments in the usual low ripple configuration are shown. Open symbols are measurements in the plasma core (r/a=0.1-0.39), while solid symbols are from the edge (r/a~0.8).